Generalized Method to Control Coupled-oscillator System Using Multi-linear Feedback

Takeshi Kano* and Shuichi Kinoshita

Graduate School of Frontier Biosciences, Osaka University, Suita 565-0871, Japan
E-mail address: takesik@fbs.osaka-u.ac.jp

(Received November 28, 2008; Accepted January 21, 2009)

Recently, we have proposed a method to control the dynamical behavior of coupled-oscillator system by regulating the coupling function through multi-linear feedback. In the present paper, we extend our previous theory such that it is even applicable to general systems where the coupling strengths, the observables, and the applied feedback signals are not uniform. This method does not require an individual output from each oscillator but only needs the output signals obtained from all the measurement nodes, and hence it has wide applicability. The validity of the method is confirmed through a simulation using a Bonhoeffer-van der Pol model.
Key words: Coupled-Oscillator System, Feedback Control, Phase Model, Coupling Function

1. Introduction

Recently, we have proposed a new method to control the dynamical behavior of coupled-oscillator system, in which various dynamical states such as desynchronization and clustering of the oscillators are obtainable (Kano and Kinoshita, 2008). In this method, we have considered a phase model (Kuramoto, 1984; Pikovsky *et al*., 2001; Manrubia *et al*., 2004) and have employed multi-linear feedback to control the functional form of the coupling function, which characterizes the dynamical behavior of coupled oscillators.

Actually, controlling dynamical behaviors of coupled oscillators has been a challenging topic owing to various practical demands (Beer *et al*., 1997; Tass, 1999; Calvitti and Beer, 2000; Klavins and Koditschek, 2002; Rosenblum and Pikovsky, 2004a, b; Hauptmann *et al*., 2005a, 2005b, 2007; Popovych *et al*., 2005, 2006; Pyragas *et al*., 2007; Kiss *et al*., 2007; Kori *et al*., 2008). For example, electrical stimulation techniques, which are known as a therapy to several neural diseases such as Parkinson's disease and essential tremor, are now developing so that the electrical stimulation desynchronizes or locally synchronizes the pathological activities of neurons effectively (Tass, 1999; Rosenblum and Pikovsky, 2004a, b; Hauptmann *et al*., 2005a, 2005b, 2007; Popovych *et al*., 2005, 2006; Pyragas *et al*., 2007). Another example is found in the field of technology. Many tasks in robotics require cyclic actions to be coordinated, such as walking, juggling, and factory automation, and hence, there is a need for stabilizing a desired phase relationship of cyclic units in robots (Beer *et al*., 1997; Calvitti and Beer, 2000; Klavins and Koditschek, 2002).

The method we have proposed previously (Kano and Kinoshita, 2008) becomes a breakthrough for the control of coupled oscillators. In fact, our method has several advantages as compared with those proposed so far (Beer *et al*., 1997; Tass, 1999; Calvitti and Beer, 2000; Klavins and Koditschek, 2002; Rosenblum and Pikovsky, 2004a, b; Hauptmann *et al*., 2005a, 2005b, 2007; Popovych *et al*., 2005, 2006; Pyragas *et al*., 2007; Kiss *et al*., 2007; Kori *et al*., 2008). First, since our method is based on the phase model and the coupling function is well controlled up to the higher Fourier harmonics, various complex behaviors are obtainable by applying small feedback signals without knowing detailed mechanisms of systems. Second, in our method, we do not need to measure an individual output from each oscillator, but only measure sum of the outputs from all the oscillators. This is extremely important because it is often practically difficult to measure individual outputs and to process them rapidly, particularly when the number of oscillators is large, as in neuronal systems.

However, our previous method still has a drawback: it is applicable only in a special case where the oscillators are coupled to each other by the same coupling strength (global coupling) and an observable is measured uniformly from all of the oscillators, with feedback signals applied uniformly to them. In actual systems, however, the coupling strengths, observables, and applied feedback signals are not generally uniform. Hence, it is clearly needed to generalize our method so that it is even applicable in the case where they are not uniform. In the present paper, we will derive a generalized method to control the dynamical behaviors of coupled oscillators, by extending our previous work (Kano and Kinoshita, 2008). We will also confirm the validity of the method through the simulation of one-dimensionally-arranged Bonhoeffer-van der Pol oscillators.

2. Theory

We begin with considering coupled oscillators following our previous work (Kano and Kinoshita, 2008). The coupled oscillators are generally described by

$$\dot{\mathbf{x}}_i = \mathbf{F}_i(\mathbf{x}_i) + \frac{1}{N}\sum_{j=1}^{N} \epsilon_{ij}\mathbf{P}_\mathbf{c}(\mathbf{x}_i(t), \mathbf{x}_j(t)), \qquad (1)$$

where N is the number of oscillators and $\mathbf{P_c}(\mathbf{x}_i(t), \mathbf{x}_j(t))$ denotes the coupling between the oscillators. ϵ_{ij} is a newly introduced parameter expressing the coupling strength between the ith and jth oscillators, where $N^{-1}\sum_{j=1}^{N}\epsilon_{ij}$ is assumed to be sufficiently smaller than unity. $\mathbf{F}_i(\mathbf{x}_i)$ denotes a set of functions describing a limit cycle. We assume that the frequencies of the oscillators are slightly different from each other in nature with the magnitude of the difference being characterized by ϵ_d that is smaller than $N^{-1}\sum_{j=1}^{N}\epsilon_{ij}$. Then, $\mathbf{F}_i(\mathbf{x}_i)$ is divided into a part common to all the oscillators and the deviation from it as $\mathbf{F}_i(\mathbf{x}_i) = \mathbf{F}(\mathbf{x}_i) + \epsilon_d \mathbf{f}_i(\mathbf{x}_i)$ (we assume that $\mathbf{F}(\mathbf{x}_i)$, $\mathbf{f}_i(\mathbf{x}_i)$, and $\mathbf{P_c}(\mathbf{x}_i(t), \mathbf{x}_j(t))$ are the functions of $O(1)$). Equation (1) is generally reduced to a phase model as (Kuramoto, 1984)

$$\dot{\phi}_i = \bar{\omega} + \epsilon_d \omega_i + \frac{1}{N}\sum_{j=1}^{N}\epsilon_{ij} q_c(\phi_i(t) - \phi_j(t)), \quad (2)$$

where

$$\omega_i = \frac{1}{2\pi}\int_0^{2\pi} d\theta \mathbf{Z}(\phi_i + \theta)\cdot \mathbf{f}_i(\mathbf{x}_0(\phi_i + \theta)), \quad (3)$$

and

$$\begin{aligned} &q_c(\phi_i - \phi_j) \\ &= \frac{1}{2\pi}\int_0^{2\pi} d\theta \mathbf{Z}(\phi_i + \theta)\cdot \mathbf{P_c}(\mathbf{x}_0(\phi_i + \theta), \mathbf{x}_0(\phi_j + \theta)). \end{aligned} \quad (4)$$

Here, $\mathbf{x}_0(\phi)$ denotes a point on the limit cycle at a phase ϕ, and $\bar{\omega}$ denotes the increasing rate of the phase, when the inhomogeneity $\epsilon_d \mathbf{f}_i(\mathbf{x}_i)$ and the coupling between oscillators are absent. Since the limit cycle constitutes a closed orbit, $\mathbf{x}_0(\phi) = \mathbf{x}_0(\phi + 2\pi)$ is naturally satisfied. $\mathbf{Z}(\phi) \equiv (\mathrm{grad}_{\mathbf{x}}\phi)_{\mathbf{x}=\mathbf{x}_0(\phi)}$ is called phase response function. It is noted that $|\mathbf{Z}(\phi)|$ should not be extremely large for any ϕ because the phase description is valid only when $\phi - \bar{\omega}t$ is kept almost constant during an oscillation period (Kuramoto, 1984). $q_c(\phi_i(t) - \phi_j(t))$ is called coupling function, whose functional form can be experimentally derived either by specifying the phase response function $\mathbf{Z}(\phi)$ (if the interaction $\mathbf{P_c}(\mathbf{x}_i(t), \mathbf{x}_j(t))$ is already known) (Kiss *et al.*, 2005), or by analyzing the period of one of two-coupled oscillators when they are not completely synchronized (Miyazaki and Kinoshita, 2006a, b). $q_c(\phi_i(t) - \phi_j(t))$ is expanded to Fourier series as $q_c(\phi_i(t) - \phi_j(t)) = \sum_k a_k^{(c)} \exp[\mathrm{i}k(\phi_i(t) - \phi_j(t))]$, where $a_{-k}^{(c)} = a_k^{(c)*}$ should be satisfied.

We consider a case where several measurement and stimulation nodes are placed in the system, as shown in Fig. 1. Here, we have called an element used for the measurement of the outputs from its neighborhood oscillators as "measurement node", while that used for the stimulation of the feedback signals to its neighborhood oscillators as "stimulation node". The data obtained from the measurement nodes are analyzed at the host computer and the feedback signals with time delays are applied from the stimulation nodes to the oscillators. Thus, the observables and the applied feedback signals are not uniform, in contrast to our previous work where they are uniform (Kano and Kinoshita, 2008).

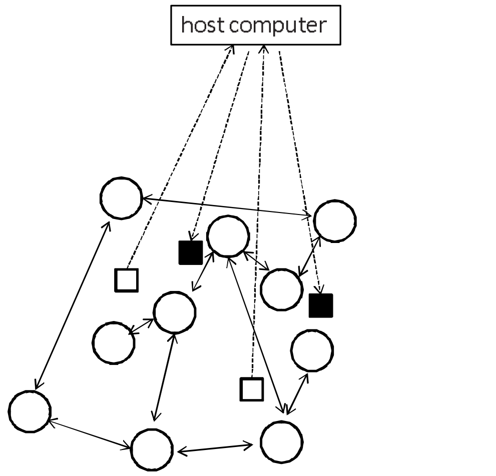

Fig. 1. Scheme of a system considered in the theory. The oscillators (empty circles) are coupled to each other ununiformly (left right arrows). The data obtained from several measurement nodes (empty squares) are analyzed at the host computer and the feedback signals with time delays are applied from the stimulation nodes (filled squares).

The model equation is then given in the following way:

$$\begin{aligned} \dot{\mathbf{x}}_i &= \mathbf{F}_i(\mathbf{x}_i) + \frac{1}{N}\sum_{j=1}^{N}\epsilon_{ij}\mathbf{P_c}(\mathbf{x}_i(t), \mathbf{x}_j(t)) \\ &\quad + \frac{1}{N}\sum_{\beta,\gamma}\epsilon'_{\beta\gamma}\rho_i^{(\beta)}\sum_{m=1}^{2M+1}\Gamma_m P_0^{(\gamma)}(t - \tau_m)\mathbf{r}, \end{aligned} \quad (5)$$

where β and γ denote indices of the stimulation and measurement nodes, respectively. $\epsilon'_{\beta\gamma}$ characterizes the rate of the output from the γth measurement node to the input to the βth stimulation node. $P_0^{(\gamma)}(t) \equiv \sum_{j=1}^{N}\sigma_j^{(\gamma)} p(\mathbf{x}_i(t))$ is the output from the γth node, where $p(\mathbf{x}_j(t))$ is an arbitrary single-valued function of $\mathbf{x}_j(t)$, and $\sigma_j^{(\gamma)}$ is a weighting factor for the measurement through the γth node. $\rho_i^{(\beta)}$ characterizes the magnitude of the feedback signal applied from the βth node to the ith oscillator. τ_m and Γ_m are the time delay and strength of the mth signal, respectively, which we will specify in the following. $\mathbf{r}$ is a unit vector whose dimension is equal to that of $\mathbf{x}_i$, and it can be selected in an arbitrary manner. The number of the feedback signals are set at $2M + 1$, where the definition of M will be described later.

Now we assume that the contribution of the third term in the right-hand side of Eq. (5) is sufficiently smaller than that of $\mathbf{F}_i(\mathbf{x}_i)$. Then, Eq. (5) is reduced to the phase model as

$$\begin{aligned} \dot{\phi}_i &= \bar{\omega} + \epsilon_d\omega_i + \frac{1}{N}\sum_{j=1}^{N}\epsilon_{ij}q_c(\phi_i(t) - \phi_j(t)) \\ &\quad + \frac{1}{N}\sum_{\beta,\gamma}\epsilon'_{\beta\gamma}\rho_i^{(\beta)} \\ &\quad \cdot \sum_{m=1}^{2M+1}\Gamma_m\sum_{j=1}^{N}\sigma_j^{(\gamma)} q_f(\phi_i(t) - \phi_j(t - \tau_m)), \end{aligned} \quad (6)$$

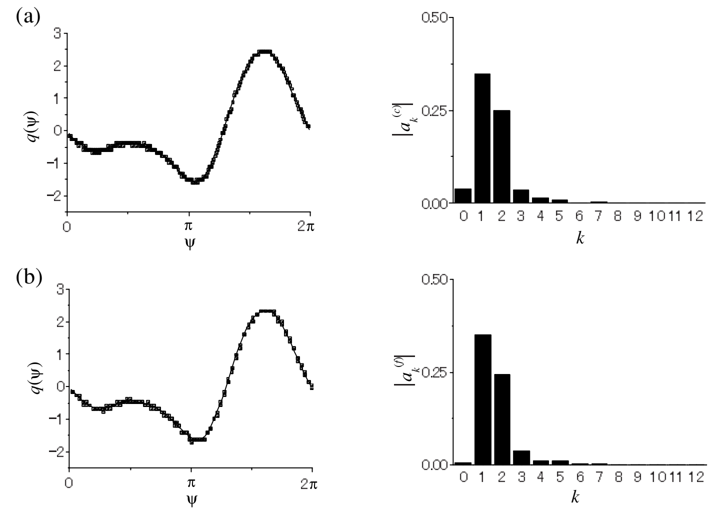

Fig. 2. Functional forms of (a) $q_c(\psi)$ and (b) $q_f(\psi)$ (left graphs). The data are obtained by using the method shown in Miyazaki and Kinoshita (2006a, b) (black dots), and they are fitted by a function $\gamma_0 + \sum_{k=1}^{12}(\beta_k \sin(k\psi) + \gamma_k \cos(k\psi))$ with the fitting parameters of β_k and γ_k (solid lines). In the right graphs, the absolute values of each Fourier coefficient, $|a_k^{(c)}|$ (or $|a_k^{(f)}|$) $= \sqrt{\beta_k^2 + \gamma_k^2}/2$ for $k \geq 1$ and γ_0 for $k = 0$, are shown.

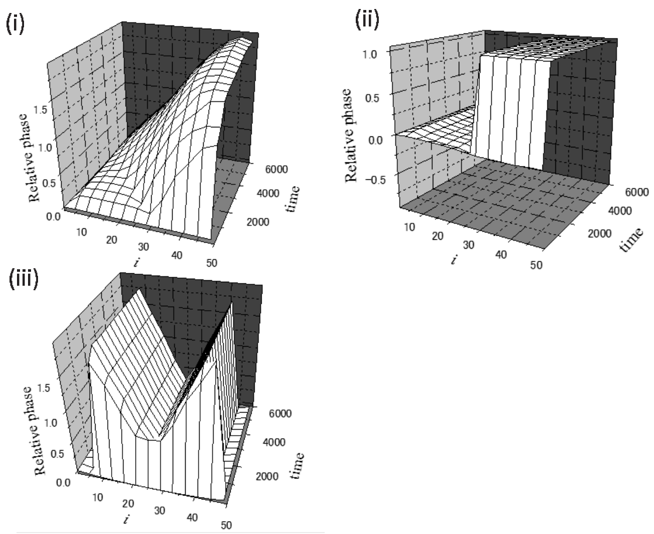

Fig. 3. Temporal evolutions of the phase difference between the ith and first oscillators obtained from the simulation of Eq. (8) when the target state is (i) unidirectional phase-shifted state, (ii) 2-cluster state, and (iii) "v-type" phase-shifted state. $\tilde{q}(\psi)$ and the positions of the nodes are given as shown in Figs. 4 and 5, respectively. The initial condition is set at $\phi_i = 0$ for all i. Since the relative phase is 2π-periodic, it is expressed within the range of (i), (iii) $[-0.05\pi, 1.95\pi]$ and (ii) $[-0.95\pi, 1.05\pi]$.

where

$$\begin{aligned}
&\sum_{j=1}^{N} \sigma_j^{(\gamma)} q_f(\phi_i(t) - \phi_j(t - \tau_m)) \\
&= \frac{1}{2\pi} \int_0^{2\pi} d\theta \mathbf{Z}(\phi_i(t) + \theta) \\
&\quad \cdot \sum_{j=1}^{N} \sigma_j^{(\gamma)} p(\mathbf{x}_0(\phi_j(t - \tau_m) + \theta))\mathbf{r}. \qquad (7)
\end{aligned}$$

The functional form of $q_f(\psi)$ can be derived in a similar manner as that of $q_c(\psi)$ (see details in Kano and Kinoshita (2008)). Let $q_f(\phi_i(t) - \phi_j(t))$ thus derived be expanded to Fourier series as $q_f(\phi_i(t) - \phi_j(t)) = \sum_k a_k^{(f)} \exp[\mathrm{i}k(\phi_i(t) - \phi_j(t))]$, where $a_{-k}^{(f)} = a_k^{(f)*}$ should be satisfied.

Suppose that Eq. (6) is consistent with the following equation:

$$\begin{aligned}
\dot{\phi}_i &= \bar{\omega} + \epsilon_d \omega_i + \frac{1}{N} \sum_{j=1}^{N} \epsilon_{ij} q_c(\phi_i(t) - \phi_j(t)) \\
&\quad + \frac{1}{N} \sum_{\beta,\gamma} \epsilon'_{\beta\gamma} \rho_i^{(\beta)} \sum_{j=1}^{N} \sigma_j^{(\gamma)} \tilde{q}(\phi_i(t) - \phi_j(t)), \qquad (8)
\end{aligned}$$

where $\tilde{q}(\psi)$ is the target coupling function. Note that the definition of this function is slightly different from that in our previous study (Kano and Kinoshita, 2008), where the natural coupling term is included into it (see equation (6) in Kano and Kinoshita (2008)). The functional form of $\tilde{q}(\psi)$ and the parameters related to the positions of the nodes, $\epsilon'_{\beta\gamma}$, $\rho_i^{(\beta)}$, and $\sigma_j^{(\gamma)}$, are explored through the simulation of

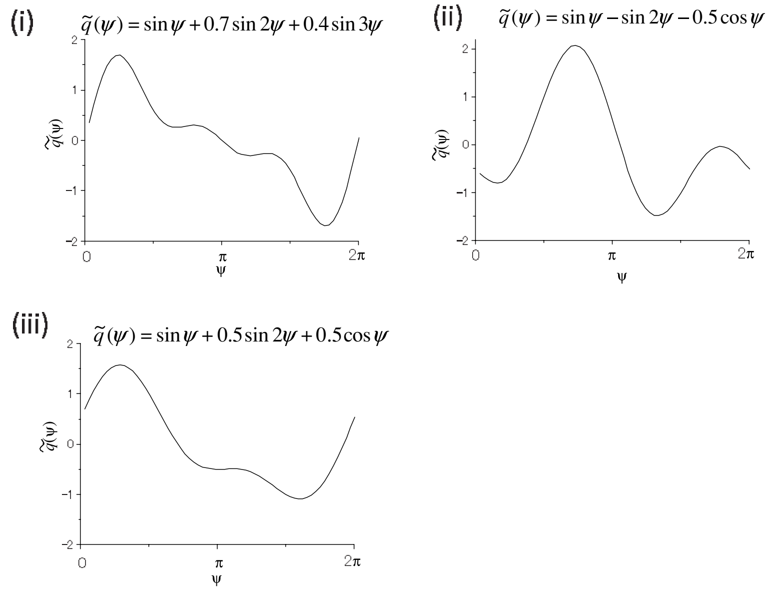

Fig. 4. Functional forms of $\tilde{q}(\psi)$ when the target state is (i) unidirectional phase-shifted state, (ii) 2-cluster state, and (iii) "v-type" phase-shifted state. Note that $\tilde{a}_k$ and $\tilde{a}_{-k}$ are set at zero when $\tilde{q}(\psi)$ does not have a Fourier component in the kth harmonic for $k \le M$, where M is taken as 8.

Eq. (8). $\tilde{q}(\psi)$ thus determined is expanded to Fourier series as $\tilde{q}(\psi) = \sum_{k=-M}^{M} \tilde{a}_k \exp[\mathrm{i}k\psi]$, where $\tilde{a}_{-k} = \tilde{a}_k^*$ should be satisfied. Here, M is defined as the highest harmonic of $\tilde{q}(\psi)$, since we aim to control the coupled oscillators with a finite number of such harmonics. It is noted that Eqs. (8) and (6) correspond to equations (6) and (8) in Kano and Kinoshita (2008), respectively, when the parameters ϵ_{ij} and $\sum_{\beta,\gamma} \epsilon'_{\beta\gamma} \rho_i^{(\beta)} \sigma_j^{(\gamma)}$ correspond to ϵ_c and ϵ_f, with the replacement of $(\epsilon_c/\epsilon_f) q_c(\phi_i(t) - \phi_j(t)) + \tilde{q}(\phi_i(t) - \phi_j(t))$ by $\tilde{q}(\phi_i(t) - \phi_j(t))$. Thus, the parameters ϵ_{ij}, $\epsilon'_{\beta\gamma}$, $\rho_i^{(\beta)}$, and $\sigma_j^{(\gamma)}$ are responsible for the extension of our previous theory (Kano and Kinoshita, 2008) to general cases.

Then, since Eq. (6) is consistent with Eq. (8), we obtain the following relation:

$$\tilde{q}(\phi_i(t) - \phi_j(t)) = \sum_{m=1}^{2M+1} \Gamma_m q_f(\phi_i(t) - \phi_j(t) + \bar{\omega}\tau_m). \quad (9)$$

Here, we have used the approximation

$$\phi_j(t - \tau_m) \approx \phi_j(t) - \bar{\omega}\tau_m, \quad (10)$$

which is applicable as far as τ_m is comparable to or shorter than the natural oscillation period because $\phi_j - \bar{\omega}t$ is kept almost constant during an oscillation period.

By comparing each Fourier coefficient of Eq. (9) up to the Mth harmonic, we obtain

$$\tilde{a}_k = \sum_{m=1}^{2M+1} \Gamma_m a_k^{(f)} e^{\mathrm{i}k\bar{\omega}\tau_m}. \quad (11)$$

Although the Fourier coefficients of the harmonics higher than M in $q_f(\psi)$ generally have non-zero values, we can minimize their contributions by taking M larger than the number of harmonics in which $q_f(\psi)$ has nonnegligible Fourier components. Equation (11) is rewritten in a matrix form as

$$\begin{pmatrix} A_0 \\ A_1 \\ A_2 \\ \vdots \\ A_M \\ B_1 \\ B_2 \\ \vdots \\ B_M \end{pmatrix} = \begin{pmatrix} 1 & 1 & \dots & 1 \\ \cos(\bar{\omega}\tau_1) & \cos(\bar{\omega}\tau_2) & \dots & \cos(\bar{\omega}\tau_{2M+1}) \\ \cos(2\bar{\omega}\tau_1) & \cos(2\bar{\omega}\tau_2) & \dots & \cos(2\bar{\omega}\tau_{2M+1}) \\ \vdots & \vdots & \ddots & \vdots \\ \cos(M\bar{\omega}\tau_1) & \cos(M\bar{\omega}\tau_2) & \dots & \cos(M\bar{\omega}\tau_{2M+1}) \\ \sin(\bar{\omega}\tau_1) & \sin(\bar{\omega}\tau_2) & \dots & \sin(\bar{\omega}\tau_{2M+1}) \\ \sin(2\bar{\omega}\tau_1) & \sin(2\bar{\omega}\tau_2) & \dots & \sin(2\bar{\omega}\tau_{2M+1}) \\ \vdots & \vdots & \ddots & \vdots \\ \sin(M\bar{\omega}\tau_1) & \sin(M\bar{\omega}\tau_2) & \dots & \sin(M\bar{\omega}\tau_{2M+1}) \end{pmatrix} \cdot \begin{pmatrix} \Gamma_1 \\ \Gamma_2 \\ \vdots \\ \vdots \\ \vdots \\ \vdots \\ \vdots \\ \vdots \\ \Gamma_{2M} \\ \Gamma_{2M+1} \end{pmatrix}, \quad (12)$$

where $A_k = \mathrm{Re}[\tilde{a}_k / a_k^{(f)}]$ and $B_k = \mathrm{Im}[\tilde{a}_k / a_k^{(f)}]$. Thus, when the values of $\tau_1, \tau_2, \dots,$ and $\tau_{2\mathrm{M}+1}$ are determined, the corresponding values of $\Gamma_1, \Gamma_2, \dots,$ and $\Gamma_{2\mathrm{M}+1}$ can be derived by solving Eq. (12).

Although there is no specified method of selecting the values of $\tau_1, \tau_2, \dots,$ and $\tau_{2\mathrm{M}+1}$, we should select them such that $\sum_{m=1}^{2M+1} |\Gamma_m|$ does not have a large value, otherwise the validity of the phase model will be lost (see details in Kano and Kinoshita (2008)). We have selected the values of $\tau_1, \tau_2, \dots,$ and $\tau_{2\mathrm{M}+1}$ in a similar manner as that in our previous study (Kano and Kinoshita, 2008). Let τ_m be set as

$$\tau_m = \frac{2\pi}{\bar{\omega}} \cdot \mathrm{frac}\left(\alpha m - \frac{\bar{\omega}\tau_0}{2\pi}\right) + \tau_0, \quad (13)$$

where $\mathrm{frac}(\alpha m - \bar{\omega}\tau_0/(2\pi))$ means the fractional part of

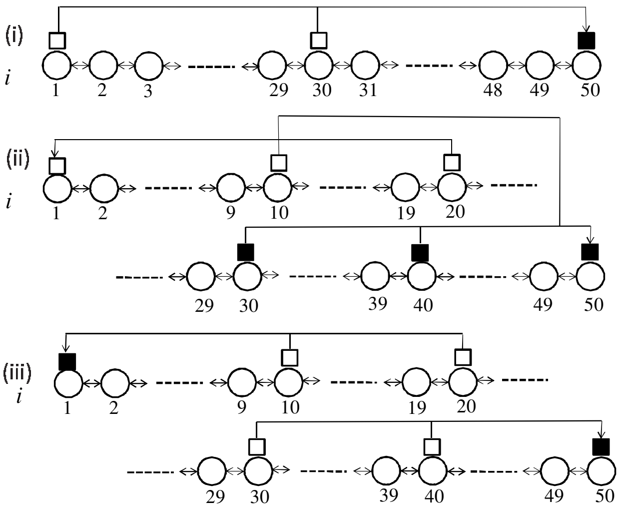

Fig. 5. Scheme of a system considered in the simulation when the target state is (i) unidirectional phase-shifted state, (ii) 2-cluster state, and (iii) "v-type" phase-shifted state. Fifty oscillators are placed in one-dimensional array and coupled to the nearest oscillators (left right arrows). Several measurement and stimulation nodes (empty and filled squares, respectively) are placed within the array so that the target state is obtained. The positions of the measurement nodes s_γ are (i) 1 and 30, (ii) 1, 10, and 20, and (iii) 10, 20, 30, and 40, whereas those of the stimulation nodes s_β are (i) 50, (ii) 30, 40, and 50, and (iii) 1 and 50. $\epsilon'_{\beta\gamma}$ is set at 0.05 when the measurement and stimulation nodes are connected by an arrow, otherwise $\epsilon'_{\beta\gamma} = 0$.

$\alpha m - \bar{\omega}\tau_0/(2\pi)$, and τ_0 is a time necessary for processing outputs, which should be comparable to or shorter than the oscillation period. Then, $\Gamma_1, \Gamma_2, \ldots,$ and Γ_{2M+1} are calculated from Eq. (12) with changing α within the range of $0 \le \alpha < 1$, and $\tau_1, \tau_2, \ldots,$ and τ_{2M+1} are systematically determined from the value of α where $\sum_{m=1}^{2M+1} |\Gamma_m|$ does not have a large value. Note that even when this scheme is used, $\sum_{m=1}^{2M+1} |\Gamma_m|$ cannot have a smaller value than the maximum value of $|A_k|$ and $|B_k|$, which can be easily proved from Eq. (12) such that $|A_k| = |\sum_{m=1}^{2M+1} \cos(k\bar{\omega}\tau_m)\Gamma_m| \le \sum_{m=1}^{2M+1} |\Gamma_m|$. Hence, $\tilde{q}(\psi)$ should be determined so that $\mathrm{Max}[|A_k|, |B_k|]$ does not have a large value.

3. Simulation

Now let us confirm the validity of this method through a simulation. Here we employ Bonhoeffer-van der Pol model, which is known as a typical model describing limit-cycle oscillations (Landa, 1996). We consider a case where the oscillators are placed in a one-dimensional array and are coupled linearly to the nearest oscillators, and several measurement and stimulation nodes are placed within the array (see Fig. 5). Then, the model equations are described as

$$\begin{pmatrix} h\dot{u}_i \\ \dot{v}_i \end{pmatrix} = \begin{pmatrix} -b_i v_i + u_i - u_i^3/3 \\ u_i + c v_i + d \end{pmatrix} + \frac{1}{N}\sum_{j=1}^{N} \epsilon_{ij}(u_j(t) - u_i(t)) \begin{pmatrix} 1 \\ 0 \end{pmatrix} + \frac{1}{N}\sum_{\beta,\gamma} \epsilon'_{\beta\gamma}\rho_i^{(\beta)} \sum_{m=1}^{2M+1} \Gamma_m P_0^{(\gamma)}(t-\tau_m) \begin{pmatrix} 1 \\ 0 \end{pmatrix}, \tag{14}$$

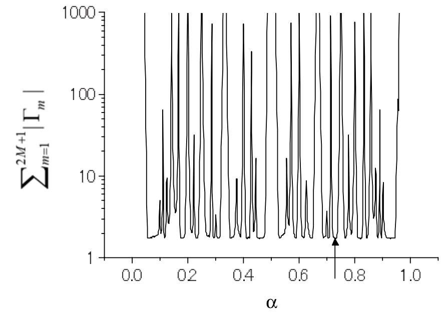

Fig. 6. α dependence of $\sum_{m=1}^{2M+1} |\Gamma_m|$ in case of $\tilde{q}(\psi) = \sin\psi + 0.5\cos\psi + 0.5\sin 2\psi$. α is changed from 0 to 1 with a step of 0.001. The minimum value of $\sum_{m=1}^{2M+1} |\Gamma_m|$ is shown by an arrow.

where the output $P_0^{(\gamma)}(t)$ is given as $P_0^{(\gamma)}(t) = \sum_{j=1}^{N} \sigma_j^{(\gamma)} u_j(t)$. The first, second, and third terms in the right-hand side denote a set of functions describing a limit-cycle, the natural coupling between the oscillators, and the feedback signals, respectively. The parameters h, b, c, and d are set at 0.2, 1, 0, and 0.8, respectively, where the natural periods of the oscillators become 4.52. The coupling strength between the ith and jth oscillators ϵ_{ij} is set at 0.25 when $j = i \pm 1$, otherwise $\epsilon_{ij} = 0$. The total number of the oscillators N is set at 50. τ_m and Γ_m are the time delay and strength of the mth feedback signal, which will be specified in the following. $\sigma_j^{(\gamma)}$ and $\rho_i^{(\beta)}$ are the weighting factors for the measurement and stimulation, respectively, and we assume that they are determined from the position dependence of the nodes as

$$\sigma_j^{(\gamma)} = \exp\left[-\frac{|j - s_\gamma|}{10}\right], \tag{15}$$

$$\rho_i^{(\beta)} = \exp\left[-\frac{|i - s_\beta|}{10}\right], \tag{16}$$

where s_γ and s_β are the positions of the γth measurement and βth stimulation node, respectively, which will be specified below. The parameter $\epsilon'_{\beta\gamma}$ will be also specified below.

In the simulation, the Runge-Kutta method is employed with the time intervals of 0.02. The initial conditions are set at $u_i = v_i = 1.5$ for all i, and hence the simulation begins with the in-phase state. In the following, we will set the target states as (i) unidirectional phase-shifted state where the phases of the oscillators are shifted unidirectionally, (ii) 2-cluster state where the oscillators are split into two synchronized subgroups whose phases are shifted to each other, and (iii) "v-type" phase-shifted state where the phases of the oscillators are shifted with the direction of the shift reversing at the center of the one-dimensional array.

To determine the feedback signals, the coupling functions $q_c(\psi)$ and $q_f(\psi)$ should be specified. They are derived by analyzing the period of one of two-coupled oscillators when they are not completely synchronized (Miyazaki and Kinoshita, 2006a, b). The obtained functional forms of $q_c(\psi)$ and $q_f(\psi)$, and their absolute values of the Fourier coefficients, $|a_k^{(c)}|$ and $|a_k^{(f)}|$, are shown in Fig. 2. We find that $|a_k^{(c)}|$ and $|a_k^{(f)}|$ decrease quickly as k increases. Hence, we select M as 8, so that it will be larger than the number

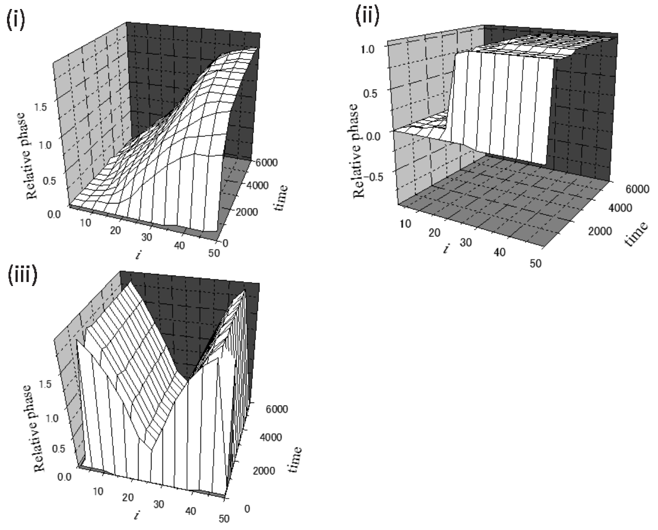

Fig. 7. Temporal evolutions of the relative phases ψ_i obtained from the simulation of Eq. (14) when the target state is (i) unidirectional phase-shifted state, (ii) 2-cluster state, and (iii) "v-type" phase-shifted state. The initial condition is set at $u_i = v_i = 1.5$ for all i. The definition of the relative phase ψ_i is described in the text. Since the relative phase is 2π-periodic, it is expressed within the range of (i)(iii) $[-0.05\pi, 1.95\pi]$ and (ii) $[-0.95\pi, 1.05\pi]$.

of the harmonics in which $q_f(\psi)$ has nonnegligible Fourier components.

The functional form of the target coupling function $\tilde{q}(\psi)$, the positions of the nodes s_γ and s_β, and the parameter $\epsilon'_{\beta\gamma}$ are selected such that the target state is obtained. They are explored through the simulation of Eq. (8) by trial and error, with taking notice that Max$[|A_k|, |B_k|]$ does not have a large value. Figure 3 shows the temporal evolutions of the phase difference between the first and ith oscillators obtained from the simulation of Eq. (8) with the initial condition of $\phi_i = 0$ for all i when $\tilde{q}(\psi)$ and the positions of the nodes are given as shown in Figs. 4 and 5, respectively. Here, $\epsilon'_{\beta\gamma}$ is set at 0.05 when the measurement and stimulation nodes in Fig. 5 are connected by an arrow, otherwise $\epsilon'_{\beta\gamma} = 0$. It is found that the target states described above are actually obtained under these conditions. $\epsilon'_{\beta\gamma}$, because changing only $\tilde{q}(\psi)$ is often insufficient to obtain the target state.

Next, the parameters τ_m and Γ_m are determined using the obtained coupling functions $q_f(\psi)$ and $\tilde{q}(\psi)$. Figure 6 shows the relation between α and $\sum_{m=1}^{2M+1} |\Gamma_m|$ obtained from Eqs. (12) and (13) in the case of $\tilde{q}(\psi) = \sin\psi + 0.5\sin 2\psi + 0.5\cos\psi$ (Fig. 4(iii)). It is found that $\sum_{m=1}^{2M+1} |\Gamma_m|$ varies significantly with α. Since we need to select the parameter sets of τ_m and Γ_m such that $\sum_{m=1}^{2M+1} |\Gamma_m|$ can be possibly minimized, we have selected them using the value of α where $\sum_{m=1}^{2M+1} |\Gamma_m|$ becomes minimum.

Then, Eq. (14) is simulated using the obtained values of τ_m and Γ_m. Figure 7 shows the temporal evolutions of the relative phases of the oscillators. Here, the relative phase of the ith oscillator ψ_i ($i = 2, 3, \ldots$, and 50) is defined as $\psi_i(t_1^{(K)}) = 2\pi(t_1^{(K+1)} - t_i^{(K')})/(t_1^{(K+1)} - t_1^{(K)}) + 2\pi n$, where n is an arbitrary integer, and $t_1^{(K)}$ and $t_i^{(K')}$ denote the time when the first and ith oscillators take maximum values of u at the Kth and K'th cycles, respectively, with K and K' satisfying $t_1^{(K)} \leq t_i^{(K')} < t_1^{(K+1)}$. It is found that the states obtained through the feedback are generally in good agreement with those obtained from the simulation of Eq. (8) (Fig. 3), although not completely. Thus, the dynamical behaviors are well controlled by the feedback.

4. Discussion

We have proposed a generalized method to control the dynamics of coupled oscillators by designing the coupling function through multi-linear feedback, and have confirmed its validity through a simulation of one-dimensionally-arranged Bonhoeffer-van der Pol oscillators. Our previous theory (Kano and Kinoshita, 2008) is only applicable to a special case where the oscillators are coupled to each other by the same coupling strength and the observable is measured uniformly from all of the oscillators with the feedback signals uniformly applied to all of them. In contrast, the present theory is even applicable to systems where the coupling strengths, the observables, and the applied feedback signals are not uniform. Such generalization is extremely important, because they are not uniform in most of actual coupled-oscillator systems. Hence, it is expected that the present method will lead to various practical applications.

The most characteristic point of the present method is that it requires only the outputs from several measurement nodes to determine the delays and the strengths of feedback signals, whereas the method reported by Kiss *et al.* (2007) and Kori *et al.* (2008) required an individual output from each oscillator. This is extremely advantageous because it is often practically difficult to measure individual outputs from all oscillators and to process them rapidly, particularly when the number of oscillators becomes large. Thus, the present method will eventually be used without practical restrictions.

When Max$[|A_k|, |B_k|]$ is large, the present method is not applicable because $\sum_{m=1}^{2M+1} |\Gamma_m|$ becomes large. Hence, $\tilde{q}(\psi)$ cannot have large Fourier components in the harmonics where $q_f(\psi)$ has small components. In spite of such restriction, in most of cases we can select $\tilde{q}(\psi)$ that leads to a target state by properly selecting the positions of the nodes, the parameter $\epsilon'_{\beta\gamma}$, the functional form of $p(\mathbf{x}_j)$, and the vector $\mathbf{r}$. Thus, the arbitrary properties of these quantities will be beneficial for expanding the applicability of the present method.

We have noticed that there exist cases where the control happens to fail. In fact, we have found that the states obtained through the feedback (Fig. 7) are not completely consistent with those obtained from the simulation of Eq. (8) (Fig. 3). The reason for such failure of the control is considered as follows. First, when the system has several stable states under the given target coupling function and positions of the nodes, it may be attracted into a state other than the target state. Second, the contribution of the fast-oscillating terms in the coupling function (see details in Miyazaki and Kinoshita (2006b)), which is eliminated due to the phase-averaging process (Eqs. (4) and (7)), may mislead to a state other than the target state. Unfortunately, it is difficult to evaluate the contribution of these terms, and hence it is still unclear in what cases the control fails at the present stage.

In conclusion, we have proposed a generalized method to control coupled oscillators by using multi-linear feedback. This method has wide applicability, and will lead to various practical applications such as the desynchronization of pathologically-activating neurons and the control of robots performing cyclic actions.

References

Beer, R. D., Quinn, R. D., Chiel, H. J. and Ritzmann, R. E. (1997) Biologically inspired approaches to robotics, *Comm. ACM*, **40**, 30–38.

Calvitti, A. and Beer, R. D. (2000) Analysis of a distributed model of leg coordination, *Biol. Cybern.*, **82**, 197–206.

Hauptmann, C., Popovych, O. and Tass, P. A. (2005a) Delayed feedback control of synchronization in locally coupled neuronal networks, *Neurocomp.*, **65**, 759–767.

Hauptmann, C., Popovych, O. and Tass, P. A. (2005b) Effectively desynchronizing deep brain stimulation based on a coordinated delayed feedback stimulation via several sites: a computational study, *Biol. Cybern.*, **93**, 463–470.

Hauptmann, C., Omel'Chenko, O., Popovych, O. V., Maistrenko, Y. and Tass, P. A. (2007) Control of spatially patterned synchrony with multisite delayed feedback, *Phys. Rev. E*, **76**, 066209.

Kano, T. and Kinoshita, S. (2008) Method to control the coupling function using multilinear feedback, *Phys. Rev. E*, **78**, 056210.

Kiss, I. Z., Zhai, Y. and Hudson, J. L. (2005) Predicting mutual entrainment of oscillators with experiment-based phase models, *Phys. Rev. Lett.*, **94**, 248301.

Kiss, I. Z., Rusin, C. G., Kori, H. and Hudson, J. L. (2007) Engineering complex dynamical structures: Sequential patterns and desynchronization, *Science*, **316**, 1886–1889.

Klavins, E. and Koditschek, D. E. (2002) Phase regulation of decentralized cyclic robotic systems, *Int. J. Robot. Res.*, **21**, 257–275.

Kori, H., Rusin, C. G., Kiss, I. Z. and Hudson, J. L. (2008) Synchronization engineering: Theoretical framework and application to dynamical clustering, *Chaos*, **18**, 026111.

Kuramoto, Y. (1984) *Chemical Oscillations, Waves, and Turbulence*, Springer-Verlag, Berlin, pp. 22–88.

Landa, P. S. (1996) *Nonlinear Oscillations and Waves in Dynamical Systems*, Kluwer Academic Publishers, Dordrecht, pp. 252–253.

Manrubia, S. C., Mikhailv, A. S. and Zanette, D. H. (2004) *Emergence of Dynamical Order: Synchronization Phenomena in Complex Systems*, World Scientific, Singapore, pp. 13–19.

Miyazaki, J. and Kinoshita, S. (2006a) Determination of a coupling function in multicoupled oscillators, *Phys. Rev. Lett.*, **96**, 194101.

Miyazaki, J. and Kinoshita, S. (2006b) Method for determining a coupling function in coupled oscillators with application to Belousov-Zhabotinsky oscillators, *Phys. Rev. E*, **74**, 056209.

Pikovsky, A., Rosenblum, M. and Kurths, J. (2001) *Synchronization: A Universal Concept in Nonlinear Sciences*, Cambridge University Press, Cambridge, pp. 222–226.

Popovych, O. V., Hauptmann, C. and Tass, P. A. (2005) Effective desynchronization by nonlinear delayed feedback, *Phys. Rev. Lett.*, **94**, 164102.

Popovych, O. V., Hauptmann, C. and Tass, P. A. (2006) Control of neuronal synchrony by nonlinear delayed feedback, *Biol. Cybern.*, **95**, 69–85.

Pyragas, K., Popovych, O. V. and Tass, P. A. (2007) Controlling synchrony in oscillatory networks with a separate stimulation-registration setup, *Europhys. Lett.*, **80**, 40002.

Rosenblum, M. G. and Pikovsky, A. S. (2004a) Controlling synchronization in an ensemble of globally coupled oscillators, *Phys. Rev. Lett.*, **92**, 114102.

Rosenblum, M. and Pikovsky, A. (2004b) Delayed feedback control of collective synchrony: An approach to suppression of pathological brain rhythms, *Phys. Rev. E*, **70**, 041904.

Tass, P. A. (1999) *Phase Resetting in Medicine and Biology: Stochastic Modelling and Data Analysis*, Springer Verlag, Berlin, pp. 265–274.